



## Evaluation of a satellite-based cyanobacteria bloom detection algorithm using field-measured microcystin data



Sachidananda Mishra <sup>a,b,\*</sup>, Richard P. Stumpf <sup>b</sup>, Blake Schaeffer <sup>c</sup>, P. Jeremy Werdell <sup>d</sup>, Keith A. Loftin <sup>e</sup>, Andrew Meredith <sup>a,b</sup>

<sup>a</sup> Consolidated Safety Services Inc., Fairfax 22030, USA

<sup>b</sup> National Oceanic and Atmospheric Administration, National Centers for Coastal Ocean Science, Silver Spring 20910, USA

<sup>c</sup> Center for Environmental Measurement and Modeling, U.S. Environmental Protection Agency, Durham 27709, USA

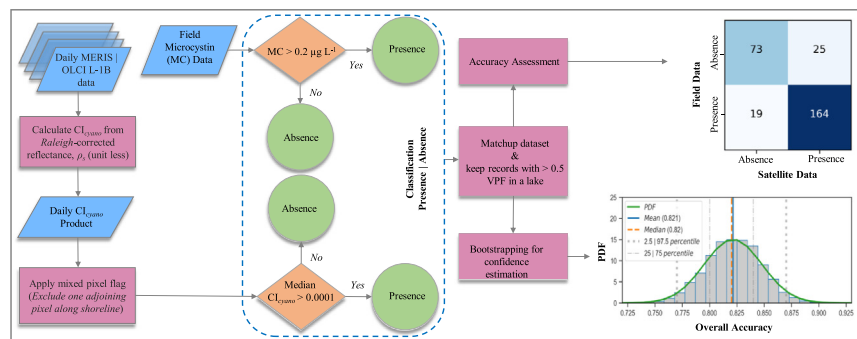
<sup>d</sup> Ocean Ecology Laboratory, NASA Goddard Space Flight Center, Greenbelt 20771, USA

<sup>e</sup> U.S. Geological Survey, Organic Chemistry Research Laboratory, Kansas Water Science Center, Lawrence 66049, USA

### HIGHLIGHTS

- Cyanobacteria Index algorithm was validated for its ability to detect CyanoHABs.
- Field microcystins data from 30 lakes in United States were used as CyanoHAB indicator.
- Algorithm detected CyanoHABs with 84% accuracy with ~90% positives correctly classified.
- The  $\text{Cl}_{\text{cyano}}$  detections could be used as a pre-screening tool to assist managers.
- Systematic approach for future validation efforts is proposed.

### GRAPHICAL ABSTRACT



### ARTICLE INFO

#### Article history:

Received 16 November 2020

Received in revised form 20 January 2021

Accepted 24 January 2021

Available online 30 January 2021

Editor: Jay Gan

#### Keywords:

CyanoHAB

Lake water quality

Cyanotoxin

Cyanobacteria index

### ABSTRACT

Widespread occurrence of cyanobacterial harmful algal blooms (CyanoHABs) and the associated health effects from potential cyanotoxin exposure has led to a need for systematic and frequent screening and monitoring of lakes that are used as recreational and drinking water sources. Remote sensing-based methods are often used for synoptic and frequent monitoring of CyanoHABs. In this study, one such algorithm – a sub-component of the Cyanobacteria Index called the  $\text{Cl}_{\text{cyano}}$ , was validated for effectiveness in identifying lakes with toxin-producing blooms in 11 states across the contiguous United States over 11 bloom seasons (2005–2011, 2016–2019). A matchup data set was created using satellite data from Medium Resolution Imaging Spectrometer (MERIS) and Ocean Land Colour Imager (OLCI), and nearshore, field-measured Microcystins (MCs) data as a proxy of CyanoHAB presence. While the satellite sensors cannot detect toxins, MCs are used as the indicator of health risk, and as a confirmation of cyanoHAB presence. MCs are also the most common laboratory measurement made by managers during CyanoHABs. Algorithm performance was evaluated by its ability to detect CyanoHAB ‘Presence’ or ‘Absence’, where the bloom is confirmed by the presence of the MCs. With same-day matchups, the overall accuracy of CyanoHAB detection was found to be 84% with precision and recall of 87 and 90% for bloom detection. Overall accuracy was expected to be between 77% and 87% (95% confidence) based on a bootstrapping simulation. These findings demonstrate that  $\text{Cl}_{\text{cyano}}$  has utility for synoptic and routine monitoring of potentially toxic cyanoHABs in lakes across the United States.

© 2021 The Author(s). Published by Elsevier B.V. This is an open access article under the CC BY license (<http://creativecommons.org/licenses/by/4.0/>).

\* Corresponding author at: Consolidated Safety Services Inc., Fairfax 22030, USA.

E-mail address: [sachi.mishra@noaa.gov](mailto:sachi.mishra@noaa.gov) (S. Mishra).

## 1. Introduction

Cyanobacterial harmful algal blooms (CyanoHABs) are widely recognized as serious water quality and public health issues. Several species of bloom-forming cyanobacteria produce cyanotoxins that can cause adverse effects on human and animal health such as hepatotoxins, neurotoxins, and dermatotoxins. Of these cyanotoxins, Microcystins (MC), a hepatotoxin, are the most commonly measured and reported (Loftin et al., 2016). MCs are commonly produced by the genera, *Dolichospermum* (*Anabaena*), *Pseudanabaena*, *Aphanizomenon*, *Microcystis*, and *Planktothrix* (Chorus and Bartram, 1999; Loftin et al., 2016) and have been detected in freshwater (coastal and lake) environments across the world, and individual reports have indicated a potential increase since the early 2000s (Preece et al., 2017). The spatial spread and intensity of CyanoHABs are suggested to be increasing globally over the past several decades (Paerl and Paul, 2012; Tararu et al., 2015) and are expected to increase in the future as a result of an increase in surface water temperature and vertical stratification (Paerl and Huisman, 2009), as well as from changes in agricultural practices (King et al., 2015; Michalak et al., 2013; Paerl et al., 2011). The National Lakes Assessment survey of 2012 (NLA-2012) - a large nationwide survey of 1038 lakes randomly selected to represent 111,818 lakes across the United States (U.S.) - assessed their biological, chemical, physical, and recreational conditions and provided a snapshot of their CyanoHAB conditions (USEPA, 2016). The NLA-2012 found MCs in 39% of the lakes in the same survey (USEPA, 2016). The NLA-2012 classified 15% of the lakes (16,773 lakes in total) as degraded or the most disturbed condition, 23% (25,718 lakes in total) as the moderately disturbed condition; and 62% (69,327 of lakes in total) as the least disturbed condition (USEPA, 2016). Such NLA surveys provide much-needed information for efficient lake management but are conducted every 5 years. A yearly assessment of individual lakes will aid in developing management strategies (Mishra et al., 2019).

There is a need for systematic and frequent screening and monitoring of lakes and water bodies that are used as recreational and drinking water sources in order to track CyanoHABs exposure to the environment, humans, and animals. Lake assessments using traditional field sampling methods are expensive, time-consuming, and often not feasible to carry out in a systematic manner. However, satellite-based remote sensing methods exist for the detection of cyanobacteria in water bodies (Binding et al., 2012; Hu et al., 2010; Matthews and Odermatt, 2015; Mishra et al., 2013; Shi et al., 2017; Simis et al., 2005; Stumpf et al., 2012; Wynne et al., 2010). Several studies have used remote sensing tools to monitor the current status of CyanoHABs in numerous larger water bodies on a routine basis (Stumpf et al., 2012; Wynne et al., 2010; Wynne et al., 2013). Several recent studies focused on developing methods to quantify key bloom metrics such as CyanoHAB magnitude (Mishra et al., 2019), spatial extent ( $\text{km}^2$ ) (Urquhart et al., 2017), temporal frequency (Clark et al., 2017), and percentage of lakes with CyanoHAB (Coffer et al., 2020).

Although there are several algorithms available for detecting and quantifying CyanoHABs, here we focus on the Cyanobacteria Index ( $\text{CI}_{\text{cyano}}$ ) algorithm (Lunetta et al., 2015; Wynne et al., 2008). The  $\text{CI}_{\text{cyano}}$  algorithm was initially developed in western Lake Erie but has since been assessed (Clark et al., 2017; Lunetta et al., 2015) in eight eastern U.S. states across New England (Connecticut, Massachusetts, Maine, New Hampshire, Rhode Island, and Vermont), Ohio, and Florida.  $\text{CI}_{\text{cyano}}$  has also been assessed for detecting cyanobacterial blooms and estimating biomass ( $\text{cells mL}^{-1}$ ) in several other areas, including Lake Balaton in Hungary and the Caspian Sea (Moradi, 2014; Palmer et al., 2015). Estimation of cyanobacteria bloom phenology using the  $\text{CI}_{\text{cyano}}$  algorithm was demonstrated across U.S. climatic regions (Coffer et al., 2020), and 25 state health advisories were used for initial 'Presence/Absence'-type validation across select lakes (Schaeffer et al., 2018). However, validation of the algorithm for larger spatial and

temporal scale 'Presence/ Absence' monitoring in the USA is still needed to evaluate the robustness of the approach.

Field data measurements pertaining to CyanoHAB confirmation often vary substantially by monitoring programs, agencies, and academic research groups. Cyanobacteria cell density ( $\text{cells mL}^{-1}$ ), biovolume ( $\text{mm}^3 \text{L}^{-1}$ ), and colony counts (colony units  $\text{mL}^{-1}$ ) would be direct measures of CyanoHAB presence but these are infrequently measured. Similarly, phycocyanin (PC) pigment concentration data, a characteristic photosynthetic pigment in cyanobacteria, has been rarely measured, although PC fluorescence instruments are becoming more common (Bastien et al., 2011; McQuaid et al., 2011; Seppala et al., 2007). MCs are the most common group of toxins that are produced by cyanobacteria (Graham et al., 2008) and their measurement directly addresses public health risks. Accordingly, the concentration ( $\mu\text{g L}^{-1}$ ) of MCs is the most commonly measured CyanoHAB indicator for evaluating risk from exposure to cyanotoxins. Although MCs cannot be detected directly by optical remote sensing, the importance of MCs for public health monitoring makes them well-suited to be a CyanoHAB indicator. Accordingly, MCs are used as the indicator of CyanoHAB presence in this study. While the  $\text{CI}_{\text{cyano}}$  algorithm uses cyanobacterial cell density or cyanobacterial chlorophyll-a (Chl-a) biomass to quantify CyanoHABs (Lunetta et al., 2015; Moradi, 2014; Palmer et al., 2015; Stumpf et al., 2012), the validation strategy implemented here was purposefully designed to evaluate the algorithm's capability to detect, rather than quantify, CyanoHABs. Performance assessment of the  $\text{CI}_{\text{cyano}}$  algorithm against MC data addresses two practical needs: (1) the usefulness of the algorithm for detecting CyanoHABs that may be toxin-producing, which is an environmental or health managers' concern; and (2) MC is the most common CyanoHAB representative field data that is consistently measured across several states and available to us to carry out this study. This approach also provides an answer to a basic question – how accurate is the  $\text{CI}_{\text{cyano}}$  at differentiating 'Presence' and 'Absence' of a CyanoHAB?

Our goal in this research is to compare the correspondence between CyanoHAB 'Presence/Absence' information from field and satellite observations. Accuracy of the  $\text{CI}_{\text{cyano}}$  product was evaluated based on the criteria that when field-measured MCs are present anywhere in a lake, the  $\text{CI}_{\text{cyano}}$  retrievals are expected to indicate the presence of cyanobacteria. The primary objective of this study was to develop a satellite data product validation strategy, based on CyanoHABs 'Presence/Absence' detection, to assess the accuracy and robustness of  $\text{CI}_{\text{cyano}}$  products in the contiguous United States.

## 2. Data and methods

### 2.1. Field microcystins data

As described in the introduction, MCs were used as the indicator of CyanoHAB presence. Measurements of microcystin concentrations were retrieved from 11 states: Washington, California, Utah, Kansas, Nebraska, Iowa, Minnesota, Ohio, Florida, New York, Vermont (Fig. 1). Field MC measurements were assembled from respective state monitoring programs and publicly accessible state CyanoHAB websites. Data tables were downloaded and merged after standardizing them to a common format. In addition to MC concentrations, some states also recorded other CyanoHAB parameters such as photosynthetic pigment concentrations, cell counts, and most abundant phytoplankton communities. However, MC was the common CyanoHAB indicator across all available datasets.

All field data sources used different methodologies for field sampling and quantification of MC concentrations. Cyanobacterial toxins such as MCs can occur in both particulate (intracellular) and dissolved phases depending on the health status of toxin-producing cyanobacteria. The particulate phase comprises the intracellular compounds, whereas the dissolved phase comprises extracellular compounds that have been released into the water column either actively by healthy cells or passively

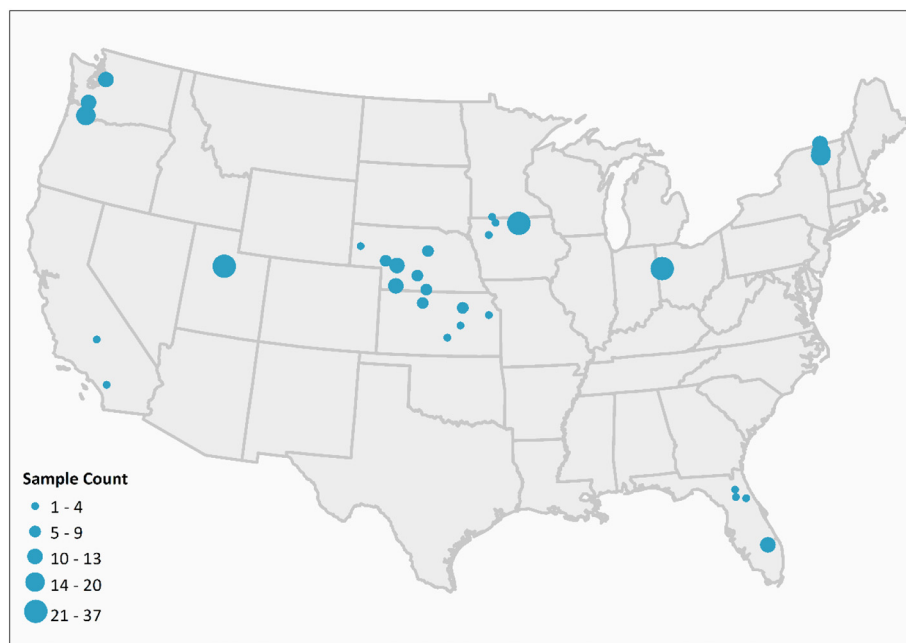


**Fig. 1.** The location map of field-measured MC samples ( $n = 281$ ) from the lakes located in 11 states across the contiguous United States. Each bubble represents a lake, and bubble size is proportional to the microcystins sample count in each lake in the matchup dataset.

upon cell lysis and death (Graham and Jones, 2007; Graham et al., 2008; Jones and Korth, 1995). Based on our review of available field data, state agencies typically measure the total MC concentrations by lysing cells in whole water, then using the Enzyme-Linked Immunosorbent Assay (ELISA) method on the lysate.

As an example, the protocol that was followed for sample collection and laboratory analysis in the Nebraska data set is described here, because several samples in the matchup data come from Nebraska. Surface samples were collected weekly on Monday and Tuesday from public lakes by the Nebraska Department of Environment and Energy (NDEE) and delivered to the laboratory. On Wednesday, lake samples were frozen and thawed three times to lyse the cyanobacterial cells and release the toxins (Walker et al., 2008). After the freeze-thaw lysing, the samples were analyzed on Thursday using ELISA laboratory test kits (Abraxis LLC.) for measuring all MCs (dissolved or free MC plus cell-bound) congeners but not limited to MC-LR. In contrast to Nebraska, other states used strip tests to screen water samples for subsequent analysis with ELISA (e.g. Utah and Vermont). Most of the MC strip tests are intended for qualitative screening of microcystins and Nodularins in recreational waters and can occasionally be unreliable (Aranda-Rodriguez and Jin, 2011). When a strip test-based positive sample was not confirmed by a follow-up ELISA test, the sample was excluded from the validation exercise. *In situ* measurements were used as supplied, however there are expected variations due to differences in toxin extraction protocols, and analytical method specificity, accuracy, and precision. Additional data such as cyanobacteria cell counts were used when available. Samples that recorded zero MC or the MC concentration was below the minimum detection level (MDL) but had cyanobacteria cell counts, then those were treated as cyanobacteria 'Presence'. In total, 34 out of 281 records (or 12%) across Florida ( $n = 9$ ), Vermont ( $n = 15$ ), Utah ( $n = 6$ ) and Washington ( $n = 4$ ) were converted from non-detect to bloom 'Presence' when cyanobacteria cell density was greater than  $10,000 \text{ cells mL}^{-1}$  (Lunetta et al., 2015).

## 2.2. Satellite data

Medium Resolution Imaging Spectrometer (MERIS) (ESA, 2020a) and Ocean Land Colour Imager (OLCI) (ESA, 2020b) Level-1B (L1B)

datasets were acquired from the NASA Ocean Biology Processing Group (OBPG, 2020) at Goddard Space Flight Center (GSFC). Spectral surface reflectances ( $\rho_s(\lambda)$ ; unitless) were calculated using l2gen (SeaDAS, 2021), the NASA standard software for processing L2 ocean colour data, then projected to an Albers projection. Briefly,  $\rho_s(\lambda)$  are determined by removing Rayleigh radiances and gaseous transmission effects that are corrected for elevation from the instrument-observed top-of-atmosphere radiances, followed by conversion to reflectance via  $\pi$  and normalization to downwelling irradiance at the sea surface. Clouds are masked using a cloud detection algorithm (Wynne et al., 2018). In order to avoid land adjacency issues, including mixed land/water pixels, adjoining pixels along each water body were discarded to ensure the signals originating from land vegetation were identified and excluded from further analysis (Urquhart and Schaeffer, 2020).

## 2.3. Cyanobacteria Index ( $Cl_{cyano}$ ) algorithm

$Cl_{cyano}$  algorithm is a spectral shape-based algorithm (Stumpf and Werdell, 2010; Wynne et al., 2008) that measures the reflectance peak height at a central wavelength of interest and is presented as:

$$SS(\lambda) = \rho_s(\lambda) - \rho_s(\lambda_-) + \{\rho_s(\lambda_-) - \rho_s(\lambda_+)\} \frac{(\lambda - \lambda_-)}{(\lambda_+ - \lambda_-)}, \quad (1)$$

where  $\lambda$  is the central band, and  $\lambda_+$  and  $\lambda_-$  are the adjacent reference bands. The Cyanobacteria Index (CI) is calculated as  $CI = -SS(681)$  (with  $\lambda_-$  and  $\lambda_+$  as 665 and 709 nm, respectively). For more specific identification of cyanobacteria, an SS(665) using 620, 665, and 681 nm is used to further confirm the presence of PC, a characteristic pigment in this taxonomic division with identifying features in this spectral region (Lunetta et al., 2015; Matthews and Odermatt, 2015; Simis et al., 2005). PC absorbs less light than Chl-a, so a higher PC concentration is needed in order to alter the spectral shape. In low concentration blooms, absorption of light at 620 nm by PC pigment concentration may not be large enough to detect the presence of cyanobacteria. A detailed explanation of the  $Cl_{cyano}$  algorithm and its ability to detect cyanobacteria is available elsewhere (Coffer et al., 2020; Lunetta et al., 2015; Mishra et al., 2019; Stumpf et al., 2016; Stumpf et al., 2012).

## 2.4. Field and satellite data matchup

Regarding the field measurements, multiple laboratory experiments have identified the MDL of MC measurements using the ELISA method to be  $0.2 \mu\text{g L}^{-1}$  (Chu et al., 1990; WHO, 2003). Additional field data sources also reported the MDL of MC to be approximately  $0.2 \mu\text{g L}^{-1}$ . Therefore, a threshold MDL of  $0.2 \mu\text{g L}^{-1}$  was chosen to ensure consistency across datasets from multiple sources. Using this threshold with field-measured MCs data, we created two classes: 1) cyanobacteria 'Presence', when MCs  $\geq 0.2 \mu\text{g L}^{-1}$  and 2) 'Absence' when MCs  $< 0.2 \mu\text{g L}^{-1}$ . Additionally, 34 samples with MC concentrations  $< 0.2 \mu\text{g L}^{-1}$ , but with cell densities  $> 10,000 \text{ cell mL}^{-1}$  were classified as cyanobacteria 'Presence'.

Regarding the satellite data, as the exact sample location within the lake was often not available, a lake-wide  $\text{Cl}_{\text{cyano}}$  median was used to indicate cyanobacteria 'Presence/Absence.' A lake was classified as CyanoHAB 'Absence' when there was no detectable  $\text{Cl}_{\text{cyano}}$  pixel present on a matchup date. A lake was classified as CyanoHAB 'Presence' when the median value of all detectable  $\text{Cl}_{\text{cyano}}$  pixels on a matchup date was  $> 0.0001$ , representing  $10,000 \text{ cells mL}^{-1}$  of *Microcystis*-equivalent cells (Lunetta et al., 2015; Wynne et al., 2010).

After the field and satellite CyanoHAB 'Presence' and 'Absence' datasets were assembled and merged to create the matchup dataset, one additional quality control metric was applied. If a bloom event is small in scale and represented by a single field sample, satellite imagery with significant obscurity from clouds, Sun glint, and other invalid data types is likely to miss the bloom. Therefore, as an additional quality control measure, valid pixel fraction (VPF), or the fraction of lake area covered by valid satellite data retrievals, was taken into account before including in the final matchup dataset. VPF threshold of  $> 0.5$  was considered to be a required criterion for satellite-derived data product accuracy assessment. Therefore, matchups with  $< 0.5$  VPF lakes were excluded from further analysis.

## 2.5. Classification accuracy metrics

As described earlier,  $\text{Cl}_{\text{cyano}}$  accuracy was determined by considering the algorithm performance as a binary classification approach (that is, 'Presence' or 'Absence'). This classification accuracy was examined using six different metrics (Powers, 2020) – (1) overall accuracy, (2) precision, (3) sensitivity or recall, (4)  $F_1$ -score, (5) specificity, and (6) false omission rate. For classification accuracy assessment, the overall accuracy or sum of correctly classified counts over the total sample count is often used. By definition, overall accuracy accurately describes algorithm performance only when each class category has similar sample counts. In the case of imbalanced class data - when one class (the majority class) has more samples than the other class (minority class) - overall accuracy is no longer sufficient, as the metric can be skewed towards the majority class. For example, if an algorithm classifies all samples as 'Present' in a dataset with 80% 'Presents' and 20% 'Absents', the algorithm would still attain 80% accuracy even if the performance of detecting the 'Absent' class is zero. Powers (2020) demonstrated that other metrics such as precision and recall are needed to evaluate moderately imbalanced data. Therefore, to assess the detection ability of  $\text{Cl}_{\text{cyano}}$  for a specific class, precision and recall metrics were also considered.

Individual metrics highlight the key strengths and weaknesses of the algorithm that have practical implications for cyanohabs management. Precision represents the fraction of data points assigned to the 'Present' class where there is true presence. On the other hand, recall, or sensitivity, indicates how well the 'Present' class was predicted, for example, the proportion of field (reference) CyanoHAB incidents that were detected as Cyanohabs by the algorithm. As precision addresses false 'Presents' and recall addresses false 'Absents', the F-measure, or  $F_1$  score, which considers both, provides a balanced summary of the performance of the algorithm.  $F_1$  score is calculated by combining

precision and recall into a single score by taking the harmonic mean.  $F_1$  score varies from 0 to 1, and the values can be assessed like those for precision. Specificity, or true negative rate, was used to assess what fraction of non-detect predictions are true 'Absents'. Specificity reports on the ability of the  $\text{Cl}_{\text{cyano}}$  algorithm to identify non-detect conditions. False omission rate was also used to specify the probability of false negatives in the prediction. Mathematical formulations of all six metrics are provided below.

$$\text{Overall accuracy} = \frac{TP + TN}{P + N} \quad (2)$$

$$\text{Precision} = \frac{TP}{TP + FP} \quad (3)$$

$$\text{Sensitivity or recall} = \frac{TP}{TP + FN} \quad (4)$$

$$F_1 \text{ score} = 2 \cdot \frac{\text{precision} \cdot \text{recall}}{\text{precision} + \text{recall}} \quad (5)$$

$$\text{Specificity} = \frac{TN}{TN + FP} \quad (6)$$

$$\text{False omission rate} = \frac{FN}{TN + FN} \quad (7)$$

TP and TN are the number of samples that are true positives ('Presence') and true negatives ('Absence'). FP and FN are the number of samples that are false positive ('Presence') and false negatives ('Absence'). P and N are the numbers of total positive ('Presence') and negative ('Absence') samples. P and N together represent the total number of samples in both classes or the total sample count.

## 2.6. Algorithm sensitivity to valid pixel fraction

The sensitivity of the  $\text{Cl}_{\text{cyano}}$  algorithm performance to VPF in the lakes was examined to evaluate the importance of VPF. Sensitivity analysis was carried out for different levels of VPF to find out the dependence of algorithm accuracy on valid satellite data coverage over a lake. At each VPF level (10%, 25%, 50%, and 80%), the lakes were classified as bloom 'Presence' or 'Absence' and the results were used in the accuracy assessment. Classification accuracy metrics were documented for each VPF level.

## 2.7. $\text{Cl}_{\text{cyano}}$ accuracy and confidence

Accuracy assessment in imbalanced datasets or datasets with skewed class proportion needs further attention, as described previously. In an imbalanced dataset, the class with a large proportion of samples is called a majority class, and the class with a smaller proportion of samples is called a minority class. The degree of class imbalance or skewness may vary from mild (20–40% samples in minority class) to extreme (<1% in minority class) and in between (moderate). As described in the previous section, the overall accuracy metric can be biased by the majority class. There are several approaches to handle the imbalanced class issue. In this study, a bootstrapping method was used to randomly sample an equal number of field observations from the CyanoHAB 'Presence' and 'Absence' classes to derive variance and confidence limits in the detection accuracy. Bootstrapping is a non-parametric statistical method often preferred for estimating measures of accuracy such as mean, standard deviation ( $\sigma$ ) of overall accuracy, and confidence intervals through repeated random sampling of observations with replacement and generating  $n$  bootstrap samples. No assumption on the distribution of the population (e.g. MC toxin observation instances) is made. Sampling with replacement is done iteratively to estimate the variability of the mean and variance of the

algorithm accuracy (Tibshirani and Efron, 1993). The statistical simulation provided a distribution of estimated output statistics, which allows assessment of the classification mean accuracy and confidence directly from a large population of statistical estimates from resampling.

The bootstrapping simulation was carried out by randomly drawing 98 samples with replacement from both classes in each iteration. A sample draw of 98 was chosen as that number of field samples was available in the minority class – the ‘Absence’ class. At every iteration, the overall accuracy of the  $\text{Cl}_{\text{cyano}}$  algorithm was estimated and saved. The simulation was repeated 10,000 times to generate a large simulated population. Statistical parameters such as mean, median,  $\sigma$ , 2.5, and 97.5 percentiles representing a 95% confidence interval and other standard metrics were computed.

### 3. Results and discussion

#### 3.1. Field microcystins data

Field MC data ( $n = 281$ ) were available from 30 lakes located in 11 states across the United States – Washington, California, Utah, Kansas, Nebraska, Iowa, Minnesota, Ohio, Florida, New York, Vermont (Table 1). Additional descriptive information on samples in the matchup data such as the name of the state, total sample number from a state, lake names, and the sampling years is provided in Table 1. Microcystin concentrations varied from non-detect ( $0 < 0.2 \mu\text{g L}^{-1}$ ) to  $750 \mu\text{g L}^{-1}$ ; 85% of the samples had  $< 5.29 \mu\text{g L}^{-1}$  of MC concentration. Out of 281 samples, 98 samples (35%) recorded MC below the MDL ( $0.2 \mu\text{g L}^{-1}$ ). From the satellite sensor point of view, field data from California, Minnesota, Florida, and Vermont were only matched to the OLCI time series. In the rest of the states, field data matched both the MERIS and OLCI time series.

#### 3.2. Accuracy assessment

Satellite and field observations from the matchup dataset were classified into CyanoHAB ‘Presence’ or ‘Absence’ based on the criteria as

shown in the schematic workflow diagram (Fig. 2). Accuracy of the algorithm was determined in two separate ways: 1) using MC data alone as field reference data, and 2) using MC and cyanobacteria cell density together as field reference data.

##### 3.2.1. MC as field reference data

Out of 281 samples in the matchup dataset, 203 data points were correctly classified, resulting in an overall accuracy of 72%. Analyzed by class, 130 out of 149 (about 87%) samples belonging to the CyanoHAB ‘Presence’ class were correctly classified, and 73 out of 132 (about 55%) samples belonging to the ‘Absence’ class were correctly classified (Fig. 3A, Table 2). Precision and recall for the CyanoHAB ‘Presence’ class were about 69% and 87%, respectively (Table 2). Overall, the  $\text{Cl}_{\text{cyano}}$  algorithm performed better at detecting CyanoHAB presence, as confirmed by the higher  $F_1$ -score (77%), compared to 65% for CyanoHAB absence. About 69% of the satellite-detected CyanoHABs belonged to the field-measured CyanoHAB class, which corresponds to about 31% false positives. The  $\text{Cl}_{\text{cyano}}$  algorithm performed satisfactorily by providing a higher recall score (about 87%) for the CyanoHAB ‘Presence’ class, meaning the algorithm was able to detect 87% of all CyanoHAB events that occurred in the dataset. On the other hand, the  $\text{Cl}_{\text{cyano}}$  algorithm had a specificity of about 55% and a false omission rate of about 21%, which means the  $\text{Cl}_{\text{cyano}}$  algorithm missed 21% of the ‘Presence’ class and detected them as ‘Absence’ class (false negatives).

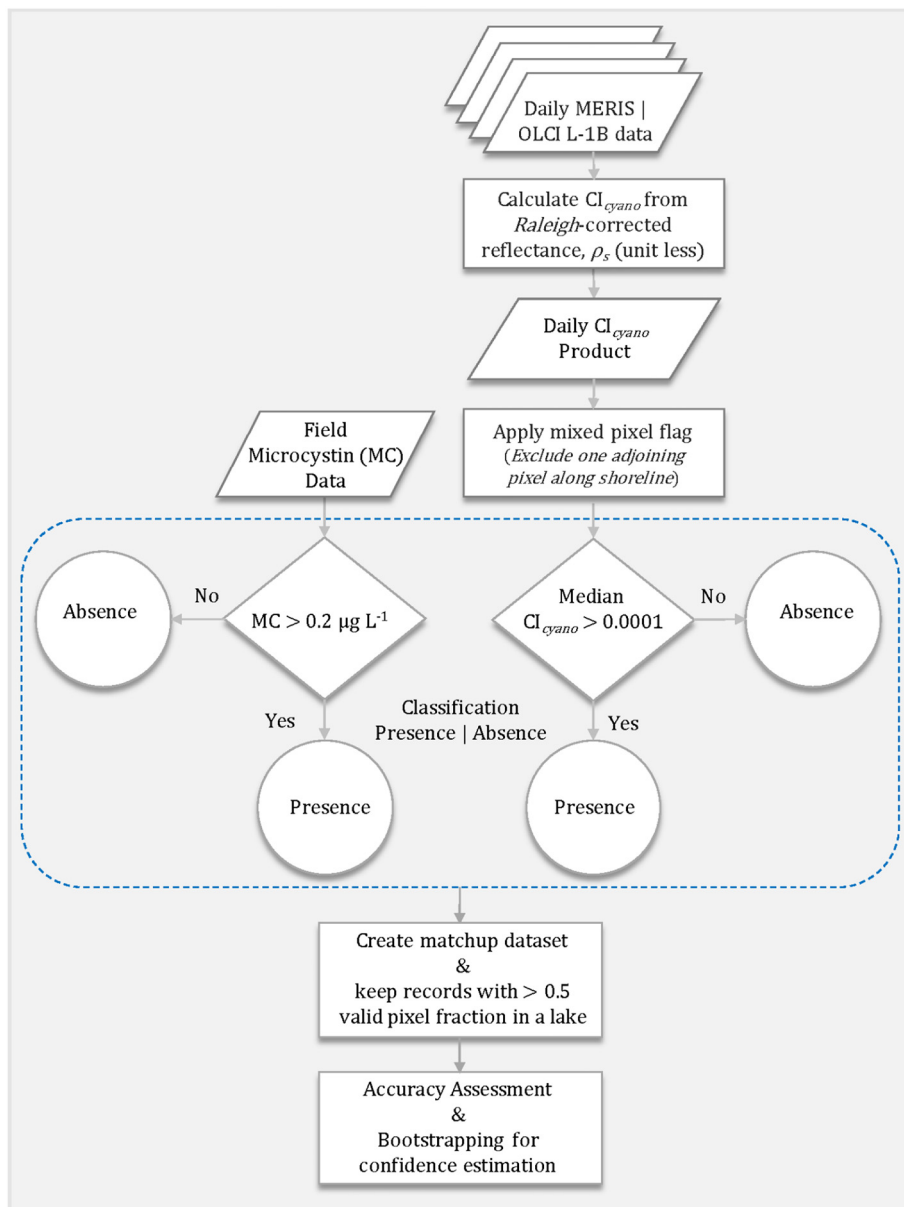
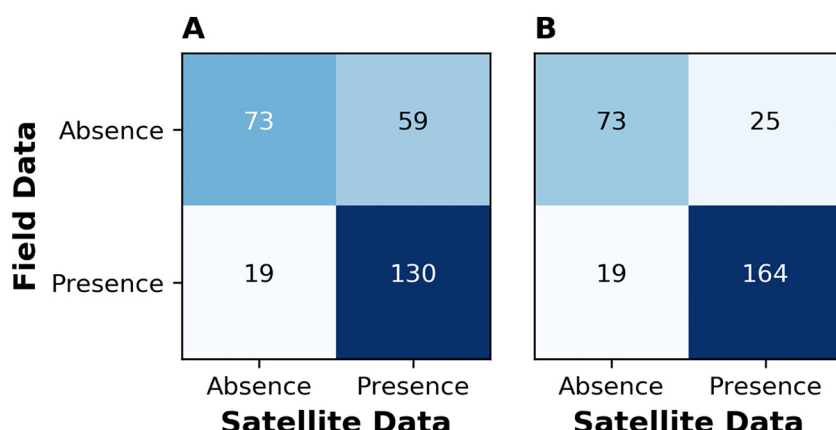
##### 3.2.2. MC and cyanobacteria cell density as field reference data

Of the 281 samples, 34 had cell density data in addition to MC concentration. When we replaced MC with cell density for those 34 samples, overall accuracy significantly improved from 72.24% to 84.34%. Out of 281 samples, 237 samples were correctly classified. By class, about 90% of the CyanoHAB ‘Presence’ class and about 74% of the ‘Absence’ class were correctly classified (Fig. 3B). The  $\text{Cl}_{\text{cyano}}$  algorithm showed better performance detecting cyanobacteria blooms (precision = 87%, recall = 90%). False positives decreased to about 13% as compared to 31% using MC-only reference data. The specificity of the algorithm improved from about 55% to 74% due to fewer numbers of false

**Table 1**

Descriptive information of field microcystins concentrations ( $\mu\text{g L}^{-1}$ ) data in lakes located in 11 states across the United States.

State	Sample count	Lake names	Sample year
California	3	• Isabella Lake	2017–2018
Florida	16	• Lake Elsinore • Lake Okeechobee • George, Lake, • Right Arm Lochloosa Lake • Santa Fe Lake	2017–2018
Iowa	31	• Clear Lake • Storm Lake • Lost Island Lake • Spirit Lake • Webster Reservoir • Marion Reservoir • Milford Lake • Cheney Reservoir • Clinton Lake • Swanson Lake • Sutherland Reservoir	2005–2006, 2008–2011, 2017–2019
Iowa, Minnesota	2	• Lake McConaughy • Johnson Reservoir	2017, 2019
Kansas	21	• Calamus Reservoir • Harlan County Lake • Lake Minatare • Mid Lake Champlain • Lake Champlain	2011, 2017–2018
Nebraska	56	• Grand Lake St Marys • Utah Lake • Lower Lake Champlain • Vancouver Lake • Silver Lake • Sammamish, Lake	2011, 2017
New York, Vermont	37		2016–2018
Ohio	37		2010, 2011, 2016
Utah	25		2016–2019
Vermont	13		2016–2018
Washington	40		2007–2011, 2017–2019

**Fig. 2.** Schematic diagram of  $\text{Cl}_{\text{cyano}}$  validation framework.**Fig. 3.** Confusion matrix from the algorithm validation with (A) MC only, and (B) MC and cyanobacteria cell density as field CyanoHAB reference data. Numbers in the confusion matrix represent the sample count in each scenario. CyanoHAB class and the no-bloom classes were coded as 'Presence' and 'Absence' class.

**Table 2** $\text{Cl}_{\text{cyano}}$  algorithm accuracy assessment metrics.

CyanoHAB Reference Data	Overall accuracy	Recall	Specificity	Precision	False omission rate	$F_1$ -score (Absence)	$F_1$ -score (Presence)
MC only	72.24%	87.25%	55.30%	68.78%	20.65%	0.65	0.77
MC, Cell Density	84.34%	89.62%	74.49%	86.77%	20.65%	0.77	0.88

positives. There was no change in the false omission rate as compared to the previous assessment. The bias towards false positives as compared to false negatives results in an outcome slightly more protective of human health. In the CyanoHAB monitoring scenario, it can be argued that it is better to have higher sensitivity or recall than higher precision and ideally zero lower false omission rate. From that aspect, the  $\text{Cl}_{\text{cyano}}$  algorithm performed well by providing a higher recall score (90%) for the CyanoHAB 'Presence' class meaning the algorithm was able to detect about 90% of all CyanoHAB events and a false omission rate of about 21% in the dataset.

### 3.2.3. Imbalanced class size and algorithm confidence

The matchup dataset contained ~65% of field CyanoHAB 'Presence' records and ~35% of 'Absence' records, which is a moderately skewed or imbalanced dataset (Fig. 4A). The overall accuracy metric may become less useful in such cases. The bootstrapping simulation (see Section 2.7) provided an approximation of the CyanoHABs 'Presence/Absence' sample population to capture our confidence in the algorithm classification accuracy. The probability density function (PDF) of the simulated population matched a normal distribution, allowing us to use that distribution to draw conclusions about the confidence interval (Fig. 4B). The mean and median of overall accuracy were found to be 82.1% and 82.0%. Based on the simulated population, overall accuracy was expected to be between 77% and 87%, with a 95% confidence, which tightly brackets the algorithm accuracy of 85% (Fig. 4B).

### 3.3. Algorithm error

To explore the false positive and false negative classes, the distribution of samples in each category in the confusion matrix (Fig. 3B) was analyzed and visualized (Figs. 5 and 6). In the false-positive prediction group, the upper-right subplot in Fig. 5, MC concentrations varied from 0.05–0.19  $\mu\text{g L}^{-1}$  in half of the samples. To put it differently, 50%

of the false positives were obtained due to how the field MC-based 'Presence/Absence' classes were defined – that is any sample with  $<0.2 \mu\text{g L}^{-1}$  was classified as non-bloom. In the remaining half of the samples,  $\text{Cl}_{\text{cyano}}$  indicated CyanoHAB 'Presence' but field data did not report a detectable MC concentration. This could be simply due to algorithmic error from inadequate masking of invalid pixels covered by haze and smoke. This could also be due to the 'Presence' of cyanobacteria that are not producing MCs. If the CyanoHABs are producing other toxins, e.g. anatoxin-a, saxitoxin, or cylindrospermospin, and not producing MCs, these cyanoHABs will not be detected by the field samples, which would result in false positives. It has been previously documented that toxin production in cyanobacteria depends on the type of strain, rather than species of cyanobacteria. One specific cyanobacterial species may have multiple strains, and toxic and non-toxic strains may co-occur in an individual lake (Graham et al., 2008; Vezie et al., 1998). This is corroborated by the 34 instances where MC was below MDL, but cyanobacteria cell density data showed the presence of cyanobacteria. When cyanobacteria cell density data was considered along with MC as CyanoHAB reference data, the total number of false positives decreased from 59 to 25 or specificity improved from about 55% to 74% (Fig. 3B, Table 2). This implies that the algorithm detects all cyanobacteria blooms, not just the toxic ones.

Similarly, in the false-negative prediction group, the lower-left subplot in Fig. 3B and Fig. 5, MC concentrations varied from 0.3–3.5  $\mu\text{g L}^{-1}$ , although 16 out of 19 samples were below 0.74  $\mu\text{g L}^{-1}$ . The false negatives may be attributed to several factors. These include: (1) the  $\text{Cl}_{\text{cyano}}$  algorithm missed the cyanobacteria presence due to algorithmic error; (2) CyanoHAB was present in a specific part of the lake but satellite data did not capture it because of either land proximity (we are masking 300 m inward) or due to obscurity from partial cloud cover, (3) MC got transported away from bloom in dissolved phase; (4) ambient MCs were detected from past blooms, but there were no cyanobacteria present at the time of the satellite overpass; (5) wind-driven vertical mixing

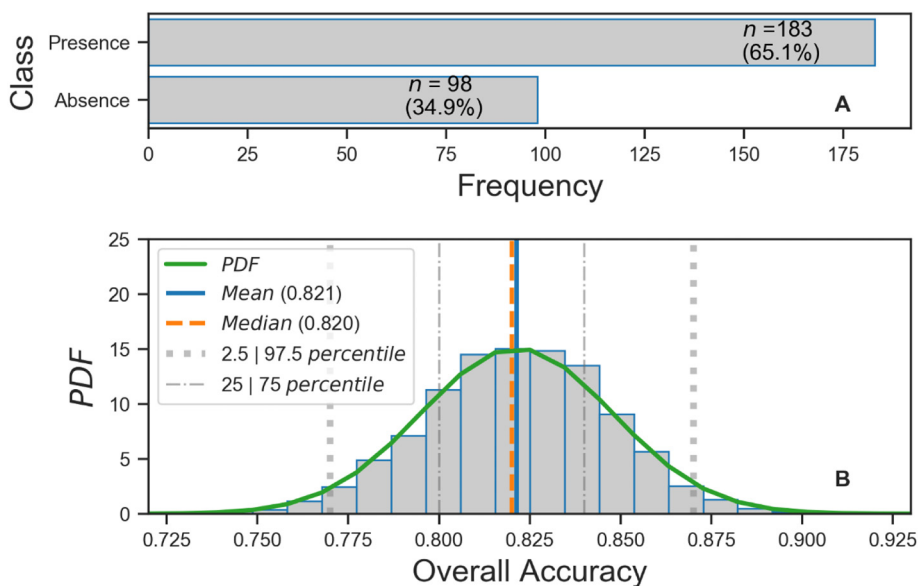


**Fig. 4.** (A) Bar plot showing class distribution in the validation dataset; (B) Distribution of overall accuracy calculated using bootstrapping method from 10,000 runs with a random draw of 98 samples. PDF is the fitted probability density function.

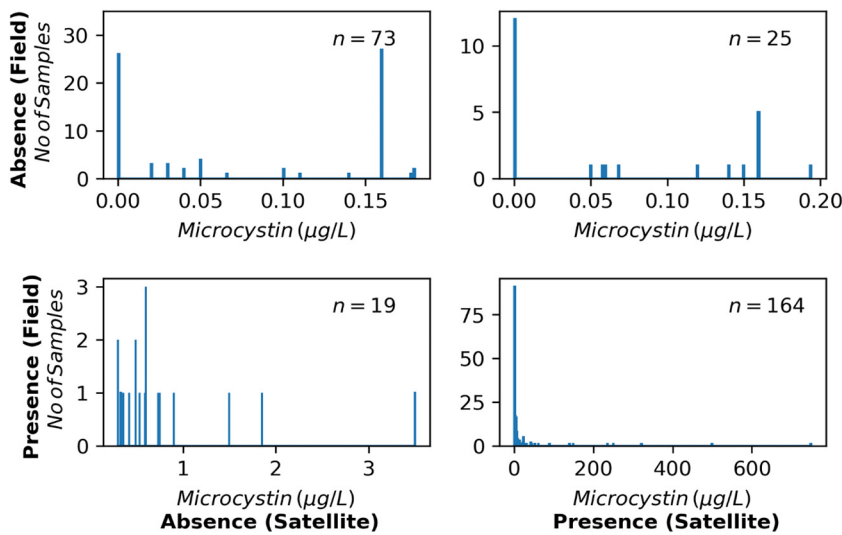


**Fig. 5.** Distribution of field microcystins samples in each of the quadrant of the confusion matrix presented in Fig. 3.

reduced surface concentrations below the satellite detection limit at the time of overpass; or, (6) the cyanobacteria were in sufficiently low concentrations to fall below the detection limit of the algorithm (which was not tuned to the ELISA MDL). For factor (6), the  $Cl_{cyano}$  algorithm uses a positive 665 nm peak height with reference to a baseline drawn from 620 nm to 681 nm to confirm cyanobacteria presence. In low concentration cyanobacteria, absorption of light at 620 nm by PC pigment is not large enough to make the 665 nm peak height positive making the cyanobacteria presence undetected. The effect of invalid or missing data in satellite observations due to cloud, Sun glint, or sensor saturation on false-negative predictions was corroborated by the results from the sensitivity analysis with respect to VPF. False omission rate or fraction of false negatives decreased with an increase in VPF, or less spatial coverage of valid satellite observation contributed to false negatives (Fig. 7).

Furthermore, studies have shown that dissolved MC released by cyanobacteria cells can stay in the water even after the termination of the bloom. MCs, especially MC-LA, are extremely stable and resistant to chemical hydrolysis or oxidation in near-neutral pH conditions as in natural waters (Bartram and Chorus, 1999). In one study, researchers

found the half-life of MC-LA to vary from 1 to 2 weeks and MC-LR half-life reaching up to 5 days (Zastepa et al., 2014). The authors in that study attributed the half-life range to differences in environmental conditions, initial MC concentrations, and physiological condition of the bloom as well as strain composition. In another study, researchers reported that the system could take 10 weeks (at pH of 1) to 12 weeks (at pH of 9) for a 90% break down of MCs (Bartram and Chorus, 1999). As a result, the presence of MCs even after termination of the bloom can make the validation strategy prone to false positives.

### 3.4. Limitations of the validation approach

As with any performance assessment, this strategy to evaluate  $Cl_{cyano}$  has limitations:

- No exact geo-locational match between field and satellite data: Due to limited field data availability, MC measurements were included even without sample collection coordinate location information. Same-day satellite estimates with greater than 50% of VPF were included. It is possible that there were CyanoHABs in a lake as recorded by

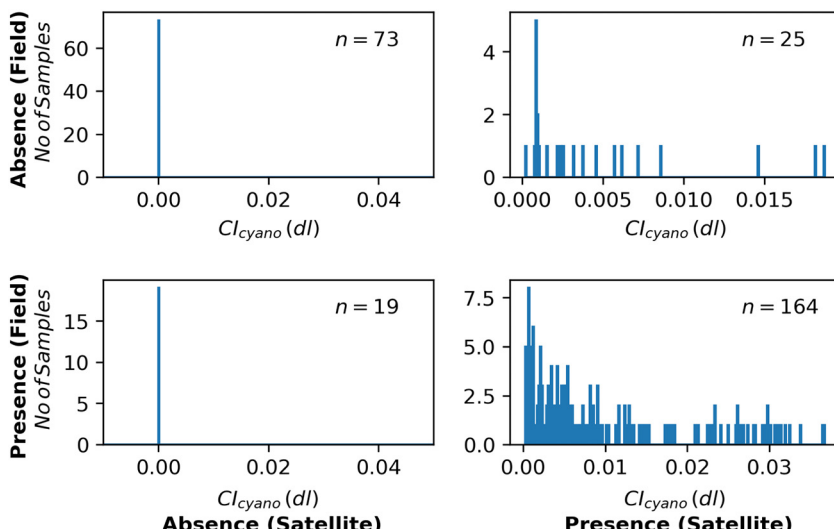


**Fig. 6.** Distribution of  $Cl_{cyano}$  (dimensionless or  $dl$ ) in each of the quadrant of the confusion matrix presented in Fig. 3.

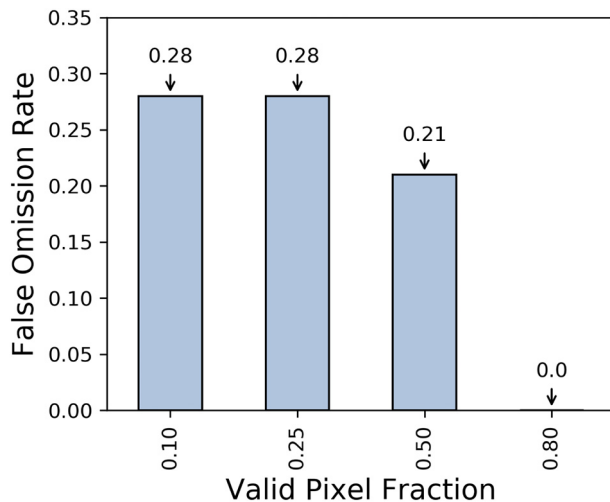


**Fig. 7.** Expected false negative prediction as a function of valid pixel fraction (VPF) in a lake.

field MC data but missed by the satellite sensor due to the presence of quality control flags such as cloud, Sun glint, land contamination, and sensor saturation.

- **Microcystins do not represent all cyanotoxins:** As they were commonly and routinely available, MC data were used as an indicator of CyanoHAB presence. Although MCs are the most common group of cyanotoxins, restricting the toxin data to MC only can increase the likelihood of artificial false positives. On the other hand, with this risk, the “false positive” may be useful for managers.
- **All cyanobacteria blooms do not produce Microcystins:** The presence of MC indicates the occurrence of cyanobacteria but the converse is not true. In a real-world scenario,  $\text{Cl}_{\text{cyano}}$  can detect many strains of cyanobacteria genera such as *Anabaena*, *Aphanizomenon*, *Cylindrospermopsis*, and *Microcystis* present in the lake that may or may not be producing MCs. This increases the odds of false positives.
- **The toxin is not what satellite sensors detect:** Photosynthetic pigments serve as an intracellular indicator of cyanobacteria biomass, which is directly detectable via satellite because of their absorption and scattering properties. Toxins may be intra and extra-cellular and do not have a known detectable optical signal. Therefore, MC from a previous bloom event may remain in the water, in the dissolved form, after the bloom has disappeared. This makes the  $\text{Cl}_{\text{cyano}}$  algorithm prone to artificial false negatives.

### 3.5. Recommendations for future CyanoHAB algorithm evaluation

Based on lessons learned from this  $\text{Cl}_{\text{cyano}}$  performance assessment in multiple states across the United States, one enhanced field data collection strategy that includes advantages and limitations of several cyanobacteria proxies is presented here to improve future related work. Thoughts on the data collection frequency for robust development and evaluation of future satellite cyanobacteria algorithms are discussed below. Each data type has limitations. As methods and technologies for data collection and analysis continue to improve, quantitative estimates will improve as well.

#### 3.5.1. Proxies of cyanobacteria as in situ reference data

Cyanotoxin concentrations (e.g., MC, anatoxin, cylindrospermopsin, saxitoxins) are ideal candidates for *in-situ* CyanoHAB monitoring (Graham et al., 2010; Loftin et al., 2016). However, cyanotoxins cannot be used for the quantitative validation of remote sensing-based cyanobacteria algorithms. Provided below is the discussion on the strengths and weaknesses of the cyanobacteria proxies and their suitability as field reference data for validating satellite algorithms.

## A. Proxies for presence/absence-type performance assessment

### 1. Visual identification

Qualitative assessment of CyanoHABs can be done through visual inspection as well as *via* digital photographs collected using hand-held digital cameras (including cellphones) or from an Unmanned Aircraft Systems (UAS) platforms. Citizen science through crowdsourcing may also result in useful data. One such example is a bloom monitoring cellphone application such as *Bloomwatch*. The *Cyanoscope* and the *Monitoring* tools available through the Cyanobacteria Monitoring Collaborative (Cyanos, 2020) also enable citizen scientists to identify, analyze, and report the occurrence of cyanobacteria bloom. Bloom confirmation data with adequate quality control can be used for ‘Presence/Absence’ type bloom performance assessment, but not for quantitative validation. Note that geographic coordinate information and observation date of the bloom event needs to be accompanied by the photographic bloom confirmation.

### 2. Field Radiometry

Direct *in situ* radiometric measurements from field spectroradiometers can be used for qualitative confirmation of cyanobacteria blooms. A distinct reflectance minimum centering at 620 nm is used as a characteristic optical signature of PC-bearing cyanobacteria and therefore *in situ* reflectance spectra can be used to confirm the presence of the cyanobacteria in a water body. Being an indirect measure of cyanobacteria presence or abundance, field radiometry data can only be used for ‘Presence/Absence’ type validation of CyanoHAB algorithms.

### 3. Cyanotoxins

Cyanotoxins such as MC, anatoxin, cylindrospermopsin, and saxitoxins are suitable proxies of CyanoHABs as these are the direct measure of toxins. However, cyanotoxins do not have meaningful optical signatures and therefore cannot be measured using remote sensing techniques. Therefore, MC concentrations can only be used for CyanoHAB ‘Presence/Absence’ detection type performance assessments, and not for quantitative validation of remote sensing cyanobacteria algorithms.

## B. Proxies for quantitative performance assessment

### 1. Chlorophyll-a concentrations

Chl-a is used for cyanobacteria bloom monitoring although it is not unique to cyanobacteria. Chl-a is the most commonly collected water quality parameter and is relatively easy to measure as standard protocols for laboratory analysis related to pigment extraction and quantification are available (Stumpf et al., 2016). For remote sensing applications, Chl-a with a stronger optical signal is a better proxy than PC when the bloom is dominated by cyanobacteria. Because Chl-a is not specific to cyanobacteria, Chl-a biomass alone cannot be used for the identification and quantification of cyanobacteria from satellite remote sensing. Taxonomic information needs to be collected as well for confirmatory identification of bloom type for the validation of satellite-derived cyanobacteria biomass.

### 2. Phycocyanin pigment concentrations

PC is considered as a characteristic photosynthetic pigment of freshwater cyanobacteria. It has been used by researchers for cyanobacteria bloom identification and quantification (Duan et al., 2012; Mishra et al., 2013; Ruiz-Verdú et al., 2008; Simis et al., 2005). PC, rather than Chl-a, is a better measure of cyanobacterial biomass when the bloom contains a mix of cyanobacteria and eukaryotic algae (Stumpf et al., 2016). However, the specific-absorption coefficient of PC at 620 nm is 2–3 times lower than the specific-absorption coefficient of Chl-a

measured at 665–681 nm (Bricaud et al., 1995; Simis et al., 2005; Stumpf et al., 2016). This leads to PC having lower sensitivity to cyanobacteria biomass and therefore lower concentrations in the early stages of the bloom formation may go undetected by satellite observations. The specific concentration of intra-cellular PC is also far more variable during a bloom than that of Chl-a (Stumpf et al., 2016). Detection of PC using satellite remote sensing can confirm the presence of cyanobacteria, but it is not an ideal proxy for CyanoHAB biomass estimation.

### 3. Phycocyanin fluorescence (*in vivo*)

PC carrying cyanobacteria produce a fluorescence signal with the maximum excitation and emission wavelengths at 620 and 650 nm, respectively. Numerous researchers have used PC *in vivo* fluorescence to quantify cyanobacteria abundance (Moldaenke et al., 2019; Seppala et al., 2007). However, *in vivo* PC fluorescence signal can be affected by water temperature and cyanobacteria morphology (Hodges et al., 2018). Biofouling is another major limiting factor reducing the reliability of the optical sensors. Therefore, PC fluorescence alone cannot be used to replace traditional microscopy-based identification and quantification method. Pigment measurements using analytical methods are needed along with PC *in vivo* fluorescence (Seppala et al., 2007).

### 4. Cyanobacteria enumeration, cell abundance, and biovolume

Identification of phytoplankton community composition using traditional methods would serve as a direct measure of cyanobacteria presence or absence. Taxonomic enumeration and cell abundance or density data (cells mL<sup>-1</sup>), biovolume (mm<sup>3</sup> L<sup>-1</sup>), and natural units (NU mL<sup>-1</sup>), which could capture colonies, filaments, and unicellular morphologies, can be used for bloom 'Presence/Absence' type validation as well as quantitative performance assessment of satellite data products. However, traditional methods such as cell counting under a microscope can have significant measurement errors of 20–30% (Chorus and Bartram, 1999). It is argued that cyanobacterial biomass or biovolume is a better indicator of the potential health risks than cell abundance (Hawkins et al., 2005). Biovolume is calculated from microscopically measured linear dimensions using geometric models, which makes the estimation of cell biovolume more challenging (Hillebrand et al., 1999). In addition to complexities such as unavailability of exact geometric models for every cell shape and difficulty in obtaining instrument measurement precision, shrinkage of cells due to preservation in Lugol's Iodine solution can add a greater source of uncertainty (up to 30–40% reduction compared to live biovolume) in estimating the biovolume of common cyanobacteria species in aquatic environments than natural variability (Hawkins et al., 2005). Similarly, colony counts can be erroneous as colonies are defined differently in different methods and colony counts may not be correlated with cyanobacteria biomass. This makes the use of cyanobacteria cell density, biovolume, and colony count data for quantitative validation of remote sensing algorithms extremely challenging.

The quantitative real-time polymerase chain reaction (qPCR) method is widely used for quantifying genes of interest, specifically cyanotoxin-producing genes, in microbial communities. qPCR could be used to estimate the total cyanobacterial biomass and the amount of potentially toxic cells (Pacheco et al., 2016). The gene copies of the 16 s rRNA gene, which are specific to the *Microcystis* genus, are quantified using qPCR-based genome copy number (equivalent to cell density) to estimate *Microcystis* cell equivalents (Baxa et al., 2010; Chaffin et al., 2019; Lu et al., 2020). Similarly, cyanotoxin-specific gene copies can be quantified to estimate the abundance of toxic strains of cyanobacteria.

All four proxies of cyanobacteria discussed above have some utility for quantitative performance assessment of satellite-based cyanobacteria quantification algorithms. However, cyanobacteria enumeration/cell abundance/biovolume are the most ideal candidates as they confirm

the presence of cyanobacteria as well as provide a direct measure of biomass or cell abundance. Moreover, the amount of Chl-a, PC, and PC-fluorescence per cell can vary dramatically with environmental conditions such as light and nutrient availability (Hillebrand et al., 1999). On the other hand, all eight cyanobacteria proxies discussed above, including cyanotoxins, field radiometry, and visual identification/citizen science-based observations, can be used for cyanobacteria bloom 'Presence/Absence' type performance assessments. Utmost quality control of all field measured data along with accurate geographic coordinates is needed to ensure high-fidelity development and assessment of satellite-derived CyanoHAB detection and/or quantification algorithms.

### 3.5.2. *In situ* data measurement frequency

*In situ* cyanobacteria monitoring samples are often collected based on bloom event response or opportunistic sampling. That leads to oversampling of CyanoHAB bloom events and under-sampling of non-bloom events that create a biased dataset of bloom and non-detects for algorithm validation. Therefore, when it is possible from the logistics and budgetary point of view, systematic sampling throughout the year would be beneficial. Otherwise, a systematic sampling over the bloom season and occasional random sampling during the non-bloom season would also be highly beneficial.

## 4. Conclusion

Frequent occurrence of CyanoHABs in lakes and reservoirs worldwide put tremendous pressure on environmental resources, public water systems, tourism, and recreational industry. Satellite remote sensing-based methods offer a frequent and systematic detection and monitoring capability for CyanoHABs that can be quite useful for efficient management of lakes and protection of environmental, animal, and human health. The Cl<sub>cyano</sub> algorithm has been used by researchers to detect and quantify cyanobacteria blooms in many geographic regions. In this study, Cl<sub>cyano</sub> bloom product generated from MERIS and OLCI sensors was evaluated and demonstrated to have about 84% accuracy of detecting CyanoHABs using MC as a proxy. The Cl<sub>cyano</sub> detections could be used as a pre-screening tool to assist managers on when and where to focus field activities to quantify toxin concentrations. Sensitivity analysis highlighted that a lake-wide valid pixel coverage of greater than 50% provides the optimal algorithm performance. The USEPA has established an MC threshold of 8 µg L<sup>-1</sup> as problematic in recreational waters (USEPA, 2019). A specific Cl<sub>cyano</sub> threshold was not derived for 8 µg L<sup>-1</sup> due to a lack of a functional relationship between the cyanobacterial biomass and cyanotoxins (Stumpf et al., 2016).

Availability of field data on cyanobacteria during both bloom and non-bloom events is one of the core challenges behind performance assessment of satellite-derived cyanobacteria data products. State agencies tend to collect water samples for laboratory analysis based on event response. As a result, the available field datasets tend to be biased towards CyanoHAB presence. Therefore, working with state agencies to establish a more systematic and routine field data sampling strategy for both cyanotoxins and cyanobacteria abundance would benefit robust future satellite algorithm calibration/validation efforts.

## Declaration of competing interest

The authors declare that they have no known competing financial interests or personal relationships that could have appeared to influence the work reported in this paper.

## Acknowledgements

This work was supported by the NASA Ocean Biology and Biogeochemistry Program/Applied Sciences Program (Grant IDs 14-SMDUNSOL14-0001, SMDSS20-0006, and 20-SMDSS20-0006) and by

U.S. Environmental Protection Agency (USEPA), National Oceanic and Atmospheric Administration (NOAA), U.S. Geological Survey Toxic Substances Hydrology Program. This article has been reviewed by the Center for Environmental Measurement and Modeling (CEMM) and approved for publication. Mention of trade names or commercial products does not constitute endorsement or recommendation for use by the U.S. Government. The views expressed in this article are those of the authors and do not necessarily reflect the views or policies of the U.S. EPA.

### CRediT authorship contribution statement

S.M. and R.P.S. conceptualized the research; S.M. and A.M. conducted data preprocessing. S.M. carried out data curation, formal processing and statistical analysis; P.J.W. provided satellite dataset; R.P.S., B.S., P.J.W., K.L., and A.M. contributed to the interpretation and discussion of the results, and S.M. wrote the paper with contributions from all authors.

### References

- Aranda-Rodriguez, R., Jin, Z., 2011. Evaluation of field test kits to detect microcystins: 2010 study. *Exposure and biomonitoring division health. Final Report 2011*, 1–21.
- Bartram, J., Chorus, I., 1999. *Toxic Cyanobacteria in Water: A Guide to their Public Health Consequences, Monitoring and Management*. CRC Press.
- Bastien, C., Cardin, R., Veilleux, É., Deblois, C., Warren, A., Laurion, I., 2011. Performance evaluation of phycocyanin probes for the monitoring of cyanobacteria. *J. Environ. Monit.* 13, 110–118.
- Baxa, D.V., Kubore, T., Ger, K.A., Lehman, P.W., Teh, S.J., 2010. Estimating the abundance of toxic *Microcystis* in the San Francisco estuary using quantitative real-time PCR. *Harmful Algae* 9, 342–349.
- Binding, C.E., Greenberg, T.A., Bukata, R.P., 2012. An analysis of MODIS-derived algal and mineral turbidity in Lake Erie. *J. Great Lakes Res.* 38, 107–116.
- Bricaud, A., Babin, M., Morel, A., Claustre, H., 1995. Variability in the chlorophyll-specific absorption coefficients of natural phytoplankton: analysis and parameterization. *Journal of Geophysical Research: Oceans* 100, 13321–13332.
- Chaffin, J.D., Mishra, S., Kane, D.D., Bade, D.L., Stanislawczyk, K., Slodysko, K.N., et al., 2019. Cyanobacterial blooms in the central basin of Lake Erie: potentials for cyanotoxins and environmental drivers. *J. Great Lakes Res.* 45, 277–289.
- Chorus, I., Bartram, J., 1999. *Toxic Cyanobacteria in Water: A Guide to their Public Health Consequences, Monitoring and Management*. CRC Press.
- Chu, F.S., Huang, X., Wei, R., 1990. Enzyme-linked immunosorbent assay for microcystins in blue-green algal blooms. *J. Assoc. Off. Anal. Chem.* 73, 451–456.
- Clark, J.M., Schaeffer, B.A., Darling, J.A., Urquhart, E.A., Johnston, J.M., Ignatius, A.R., et al., 2017. Satellite monitoring of cyanobacterial harmful algal bloom frequency in recreational waters and drinking water sources. *Ecol. Indic.* 80, 84–95.
- Coffer, M.M., Schaeffer, B.A., Darling, J.A., Urquhart, E.A., Salls, W.B., 2020. Quantifying national and regional cyanobacterial occurrence in US lakes using satellite remote sensing. *Ecol. Indic.* 111, 105976.
- Cyanos. Cyanobacteria Monitoring Collaborative. Last accessed on Jan 10, 2021 at <https://cyanos.org>, 2020.
- Duan, H., Ma, R., Hu, C., 2012. Evaluation of remote sensing algorithms for cyanobacterial pigment retrievals during spring bloom formation in several lakes of East China. *Remote Sens. Environ.* 126, 126–135.
- ESA. Explore MERIS. Last accessed on Jan 10, 2021 at <https://earth.esa.int/eogateway/instruments/meris>, 2020a.
- ESA. OLCI Instrument Payload. Last accessed on Jan 10, 2021 at <https://sentinel.esa.int/web/sentinel/missions/sentinel-3/instrument-payload/olci>, 2020b.
- Graham, J.L., Jones, J.R., 2007. Microcystin distribution in physical size class separations of natural plankton communities. *Lake and Reservoir Management* 23, 161–168.
- Graham JL, Loftin KA, Ziegler AC, Meyer MT. Guidelines for design and sampling for cyanobacterial toxin and taste-and-odor studies in lakes and reservoirs. U.S. Geological Survey, 2008.
- Graham, J.L., Loftin, K.A., Meyer, M.T., Ziegler, A.C., 2010. Cyanotoxin mixtures and taste-and-odor compounds in cyanobacterial blooms from the Midwestern United States. *Environmental science & technology* 44, 7361–7368.
- Hawkins, P.R., Holliday, J., Kathuria, A., Bowling, L., 2005. Change in cyanobacterial biovolume due to preservation by Lugol's iodine. *Harmful Algae* 4, 1033–1043.
- Hillebrand, H., Dürselen, C.D., Kirschtel, D., Pollingher, U., Zohary, T., 1999. Biovolume calculation for pelagic and benthic microalgae. *J. Phycol.* 35, 403–424.
- Hodges, C.M., Wood, S.A., Puddick, J., McBride, C.G., Hamilton, D.P., 2018. Sensor manufacturer, temperature, and cyanobacteria morphology affect phycocyanin fluorescence measurements. *Environ. Sci. Pollut. Res.* 25, 1079–1088.
- Hu C, Lee Z, Ma R, Yu K, Li D, Shang S. Moderate Resolution Imaging Spectroradiometer (MODIS) observations of cyanobacteria blooms in Taihu Lake, China. *Journal of Geophysical Research* 2010; 115.
- Jones, G.J., Korth, W., 1995. In situ production of volatile odour compounds by river and reservoir phytoplankton populations in Australia. *Water Sci. Technol.* 31, 145–151.
- King, K.W., Williams, M.R., Fausey, N.R., 2015. Contributions of systematic tile drainage to watershed-scale phosphorus transport. *J. Environ. Qual.* 44, 486–494.
- Loftin, K.A., Graham, J.L., Hilborn, E.D., Lehmann, S.C., Meyer, M.T., Dietze, J.E., et al., 2016. Cyanotoxins in inland lakes of the United States: occurrence and potential recreational health risks in the EPA National Lakes Assessment 2007. *Harmful Algae* 56, 77–90.
- Lu, J., Struewing, J., Wymer, L., Tettenhorst, D.R., Shoemaker, J., Allen, J., 2020. Use of qPCR and RT-qPCR for monitoring variations of microcystin producers and as an early warning system to predict toxin production in an Ohio inland lake. *Water Res.* 170, 115262.
- Lunetta, R.S., Schaeffer, B.A., Stumpf, R.P., Keith, D., Jacobs, S.A., Murphy, M.S., 2015. Evaluation of cyanobacteria cell count detection derived from MERIS imagery across the eastern USA. *Remote Sens. Environ.* 157, 24–34.
- Matthews, M.W., Odermatt, D., 2015. Improved algorithm for routine monitoring of cyanobacteria and eutrophication in inland and near-coastal waters. *Remote Sens. Environ.* 156, 374–382.
- McQuaid, N., Zamyadi, A., Prévost, M., Bird, D., Dorner, S., 2011. Use of in vivo phycocyanin fluorescence to monitor potential microcystin-producing cyanobacterial biovolume in a drinking water source. *J. Environ. Monit.* 13, 455–463.
- Michalak, A.M., Anderson, E.J., Beletsky, D., Boland, S., Bosch, N.S., Bridgeman, T.B., et al., 2013. Record-setting algal bloom in Lake Erie caused by agricultural and meteorological trends consistent with expected future conditions. *Proc. Natl. Acad. Sci. U. S. A.* 110, 6448–6452.
- Mishra, S., Mishra, D.R., Lee, Z., Tucker, C.S., 2013. Quantifying cyanobacterial phycocyanin concentration in turbid productive waters: a quasi-analytical approach. *Remote Sens. Environ.* 133, 141–151.
- Mishra, S., Stumpf, R.P., Schaeffer, B.A., Werdell, P.J., Loftin, K.A., Meredith, A., 2019. Measurement of cyanobacterial bloom magnitude using satellite remote sensing. *Sci. Rep.* 9, 1–17.
- Moldaenke, C., Fang, Y., Yang, F., Dahlhaus, A., 2019. Early warning method for cyanobacteria toxin, taste and odor problems by the evaluation of fluorescence signals. *Sci. Total Environ.* 667, 681–690.
- Moradi, M., 2014. Comparison of the efficacy of MODIS and MERIS data for detecting cyanobacterial blooms in the southern Caspian Sea. *Mar. Pollut. Bull.* 87, 311–322.
- OBPG N. NASA Ocean Biogeochemistry Group. Last accessed on Jan 10, 2021 at <https://oceancolor.gsfc.nasa.gov/>, 2020.
- Pacheco, A.B.F., Guedes, I.A., Azevedo, S.M., 2016. Is qPCR a reliable indicator of cyanotoxin risk in freshwater? *Toxins* 8, 172.
- Paelr, H.W., Huisman, J., 2009. Climate change: a catalyst for global expansion of harmful cyanobacterial blooms. *Environ. Microbiol. Rep.* 1, 27–37.
- Paelr, H.W., Paul, V.J., 2012. Climate change: links to global expansion of harmful cyanobacteria. *Water Res.* 46, 1349–1363.
- Paelr, H.W., Hall, N.S., Calandino, E.S., 2011. Controlling harmful cyanobacterial blooms in a world experiencing anthropogenic and climatic-induced change. *Sci. Total Environ.* 409, 1739–1745.
- Palmer, S.C.J., Odermatt, D., Hunter, P.D., Brockmann, C., Présing, M., Balzter, H., et al., 2015. Satellite remote sensing of phytoplankton phenology in Lake Balaton using 10 years of MERIS observations. *Remote Sens. Environ.* 158, 441–452.
- Powers DM. Evaluation: from precision, recall and F-measure to ROC, informedness, markedness and correlation. arXiv preprint arXiv:2010.16061 2020.
- Preece, E.P., Hardy, F.J., Moore, B.C., Bryan, M., 2017. A review of microcystin detections in estuarine and marine waters: environmental implications and human health risk. *Harmful Algae* 61, 31–45.
- Ruiz-Verdú, A., Simis, S.G., de Hoyos, C., Gons, H.J., Peña-Martínez, R., 2008. An evaluation of algorithms for the remote sensing of cyanobacterial biomass. *Remote Sens. Environ.* 112, 3996–4008.
- Schaeffer, B.A., Bailey, S.W., Conmy, R.N., Galvin, M., Ignatius, A.R., Johnston, J.M., et al., 2018. Mobile device application for monitoring cyanobacteria harmful algal blooms using Sentinel-3 satellite ocean and land colour instruments. *Environ. Model Softw.* 109, 93–103.
- SeaDAS. SeaDAS: SeaWiFS Data Analysis System. Last accessed on Jan 10, 2021 at <https://seadas.gsfc.nasa.gov/>, 2021.
- Seppala, J., Ylöstalo, P., Kaitala, S., Hällfors, S., Raateoja, M., Maunula, P., 2007. Ship-of-opportunity based phycocyanin fluorescence monitoring of the filamentous cyanobacteria bloom dynamics in the Baltic Sea. *Estuar. Coast. Shelf Sci.* 73, 489–500.
- Shi, K., Zhang, Y., Zhou, Y., Liu, X., Zhu, G., Qin, B., et al., 2017. Long-term MODIS observations of cyanobacterial dynamics in Lake Taihu: responses to nutrient enrichment and meteorological factors. *Sci. Rep.* 7, 40326.
- Simis, S.G.H., Peters, S.W.M., Gons, H.J., 2005. Optical changes associated with cyanobacterial bloom termination by viral lysis. *J. Plankton Res.* 27, 937–949.
- Stumpf, R.P., Werdell, P.J., 2010. Adjustment of ocean color sensor calibration through multi-band statistics. *Opt. Express* 18, 401–412.
- Stumpf, R.P., Wynne, T.T., Baker, D.B., Fahnsti, G.L., 2012. Interannual variability of cyanobacterial blooms in Lake Erie. *PLoS One* 7, e42444.
- Stumpf, R.P., Davis, T.W., Wynne, T.T., Graham, J.L., Loftin, K.A., Johengen, T.H., et al., 2016. Challenges for mapping cyanotoxin patterns from remote sensing of cyanobacteria. *Harmful Algae* 54, 160–173.
- Taranu, Z.E., Gregory-Eaves, I., Leavitt, P.R., Bunting, L., Buchaca, T., Catalan, J., et al., 2015. Acceleration of cyanobacterial dominance in north temperate-subarctic lakes during the Anthropocene. *Ecol. Lett.* 18, 375–384.
- Tibshirani, R.J., Efron, B., 1993. An introduction to the bootstrap. *Monographs on statistics and applied probability* 57, 1–436.
- Urquhart, E.A., Schaeffer, B.A., 2020. Envisat MERIS and Sentinel-3 OLCI satellite lake biophysical water quality flag dataset for the contiguous United States. Data in brief 28, 104826.
- Urquhart, E.A., Schaeffer, B.A., Stumpf, R.P., Loftin, K.A., Werdell, P.J., 2017. A method for examining temporal changes in cyanobacterial harmful algal bloom spatial extent using satellite remote sensing. *Harmful Algae* 67, 144–152.

- USEPA. National lakes assessment 2012: a collaborative survey of lakes in the United States. US Environmental Protection Agency Washington, DC, 2016.
- USEPA. Recommended Human Health Recreational Ambient Water Quality Criteria or Swimming Advisories for Microcystins and Cylindrospermopsin, EPA Document Number: 822-R-19-001, <https://www.epa.gov/sites/production/files/2019-05/documents/hh-rec-criteria-habs-document-2019.pdf>, Last accesses on: 08/07/2020, 2019.
- Vezie, C., Brient, L., Sivonen, K., Bertru, G., Lefevre, J.-C., Salkinoja-Salonen, M., 1998. Variation of microcystin content of cyanobacterial blooms and isolated strains in Lake grand-lieu (France). *Microb. Ecol.* 35, 126–135.
- Walker S, Lund J, Schumacher D, Brakhage P, McManus B, Miller J, et al. Nebraska experience. Cyanobacterial harmful algal blooms: state of the science and research needs. Springer, 2008, pp. 139–152.
- WHO. Cyanobacterial Toxins: Microcystin-LR in Drinking-Water Background Document for Development of WHO Guidelines for Drinking-Water Quality. 2003. World Health Organization, Geneva: Addendum to 2003; 2.
- Wynne, T.T., Stumpf, R.P., Tomlinson, M.C., Warner, R.A., Tester, P.A., Dyble, J., et al., 2008. Relating spectral shape to cyanobacterial blooms in the Laurentian Great Lakes. *Int. J. Remote Sens.* 29, 3665–3672.
- Wynne, T.T., Stumpf, R.P., Tomlinson, M.C., Dyble, J., 2010. Characterizing a cyanobacterial bloom in western Lake Erie using satellite imagery and meteorological data. *Limnol. Oceanogr.* 55, 2025–2036.
- Wynne, T.T., Stumpf, R.P., Tomlinson, M.C., Fahnstiel, G.L., Dyble, J., Schwab, D.J., et al., 2013. Evolution of a cyanobacterial bloom forecast system in western Lake Erie: development and initial evaluation. *J. Great Lakes Res.* 39, 90–99.
- Wynne, T., Meredith, A., Briggs, T., Litaker, W., Stumpf, R., 2018. Harmful algal bloom forecasting branch ocean color satellite imagery processing guidelines. NOAA Technical Memorandum NOS NCCOS 252, 48.
- Zastepa, A., Pick, F., Blais, J., 2014. Fate and persistence of particulate and dissolved microcystin-LA from *Microcystis* blooms. *Human and Ecological Risk Assessment: An International Journal* 20, 1670–1686.